Journal of Engineering Issues and Solutions

Studying the spatio-temporal changes of urban green space: A case study of Pokhara Metropolitan City

Sandip Subedi[1,2], Shiva Pokhrel[3,4,*]

[1] *Department of Geomatics Engineering, Paschimanchal Campus, IoE, Institute of Engineering, Tribhuvan University*

[2] *Pokhara Metropolitan City, Kaski, Nepal*

[3] *Center for Space Science and Geomatics Studies (CSSGS), Paschimanchal Campus, IoE, TU*

[4] *Centre for Environmental and Sustainable Agriculture Research (CESAR), Nepal*

**Corresponding email: shiva.pokhrel063@gmail.com*

Received: November 14, 2022; Revised: March 09, 2023; Accepted: March 21, 2023

doi:https://doi.org/10.3126/joeis.v2i1.49491

Abstract

Green space refers to land areas covered primarily with vegetation, including parks, gardens, nature reserves, and other similar areas. These spaces offer various benefits such as supporting biodiversity, enhancing air and water quality, promoting mental and physical well-being, providing opportunities for recreation and social interaction, and improving the overall beauty of the environment. To assess the dynamics of green space in Pokhara Metropolitan City (PMC), maximum likelihood classification and normalized difference vegetation index (NDVI) methods were utilized to analyze satellite imagery. The study showed two distinct patterns of urban green space, with the green space in the central city gradually decreasing, while the nearby suburban and remote areas of PMC experienced an increase as agricultural land was transformed into grassland due to population migration. Consequently, the area of moderately healthy vegetation increased, while healthy vegetation decreased from 4926 hectares (10.61% of total area) to 2535 hectares (5.46% of total area). Additionally, the area of no vegetation such as urban areas increased from 1.8% to 2.17%. An accuracy assessment was used to validate the analyzed data, resulting in an overall accuracy of 81.91% and a Kappa coefficient of 0.63. The primary factors contributing to the loss of green spaces were urban growth and population growth within the inner metropolis. Therefore, it is crucial to maintain PMC's green areas and give more attention to this issue while developing municipal plans and policies in the future.

Keywords: *Maximum likelihood classification, NDVI, Satellite imagery, Urban green space*

1. Introduction

Urban green spaces are defined as regions within a city that are covered in any type of green infrastructure, including parks, open fields, trees, agricultural lands, and plants beside highways (Byomkesh et al., 2012; Davies et al., 2008). A healthy ecosystem must have green places. It is referred to as the city's "lungs" since

it improves social interactions and both physical and mental health (Wolch et al., 2014). Additionally, green space helps to lessen negative environmental effects, helps to control the microclimate, and greatly promotes ecological integrity. The United Nations Environment Programme (UNEP) determined that a city in a developing area must have healthy green spaces covering at least 25% of its area (Shih, 2017). Planning for urban green areas is receiving more attention recently as its significance is recognized and it has emerged as a hot button issue for research, the economy, and urban planning (Nawar et al., 2022).

The world has become more urbanized in recent decades, with 54.4 percent of the population (UN, 2016) now residing in various types of cities and towns. Approximately 4 billion people lived in cities in 2015 according to one of the most recent projections from the United Nations Economic and Social Council (UNESC, 2017) and it has been predicted that by 2050, roughly two thirds of the population will reside in urban areas. Populations residing in most cities in developing countries are becoming more vulnerable because of rapid and unplanned urbanization and insufficient supply of basic needs and services (Morris et al., 2016; Tew et al., 2019). The unplanned urbanization process, which results in the fragmentation and diminution of green spaces and ultimately causes environmental damage, has been influenced by migration towards the city at an alarming rate. Urban temperature is impacted by green space since studies have shown that they can regulate and control temperature.

Geospatial analysis frequently uses remote sensing and the Geographic Information System (GIS). Since remotely sensed satellite data is freely available, it is easier for poorer nations to conduct analysis utilizing that data (Abebe & Megento, 2017; Pokhrel, 2019; Zhou & Wang, 2011). To determine changes in land use brought on by human activity, the normalized difference vegetation index (NDVI) is utilized (Aburas et al., 2015). Numerous research used the NDVI approach to look into changes in vegetation cover (Montandon & Small, 2008; Zhang et al., 2009). Richards claims that supervised categorization is helpful for quantitative data of imagery obtained by remote sensing (Richards, 2006). Rwanga claims that remote sensing is an essential tool for identifying land use and land cover (Rwanga & Ndambuki, 2017). Any research on remote sensing must compare the simulation to the observation. Thus, the error matrix, also known as the confusion matrix, supports the accuracy of these analyses. The Kappa coefficient evaluate how well the classification performed as compared to just randomly assigning values, i.e. did the classification do better than random so, it is a unique way to evaluate accuracy (Kuang et al., 2021).

Green space encourages carbon and oxygen balance and contributes to clean air. Additionally, it lowers the ozone level. According to research conducted in Ankara, the expansion of green spaces afforded locals more amenities and opportunities for social contact (Rukiye Duygu Çay and Fatma Aşılıoğlu, 2016). Wolch et al. (2014) contends that green space not only improves ecosystem functions but also population health. According to a study conducted in Belgium, homes with greater greenery had lower rates of respiratory disease death (Bauwelinck et al., 2021). Additionally, maintaining carbon sequencing i.e., tracking and monitoring the movement of carbon through various ecosystems and industries to help manage the impacts of carbon emissions on the environment and environmental quality measurement are encouraged by green spaces.

This study focuses on examining the spatiotemporal dynamic changes in green space within a metropolitan area, using Pokhara Metropolitan City (PMC) as a case study. The research aims to answer two key questions: (1) What is the current extent of green land in PMC? (2) How has the amount of green space changed over the past 21 years (2000-2021)? The specific objectives of the study are to identify and measure green areas within PMC and to compare their changes over time. The findings of this research will be useful for the Nepal government to formulate effective city planning and policy in the face of urbanization. Furthermore, it will enable decision-makers and researchers to evaluate the impact of urbanization and raise awareness about

the importance of conserving PMC's remaining green spaces to create a more sustainable and healthier city in the future.

2. Materials and Methods

2.1 Study area

Recently, there was a federal restructuring of Nepal, which resulted in Pokhara becoming the capital of Gandaki Province and the administrative headquarters of the Kaski district. The city is also the largest metropolitan area in the country in terms of geographical size, encompassing the former Pokhara sub-metro, Lekhnath Municipality, and nearby village development committees (VDCs) such as Bhadauri Tamagi, Kristi, Aarba, and Pumdi Bhumdi. Its total area is 464.94 km², accounting for 0.31 percent of the country's total area and representing 23.01 percent of the Kaski district. Pokhara experiences an average temperature ranging from 7°C to 31°C and has an annual rainfall of 3800 mm. As of 2011, the total population of PMC, according to Central Bureau of Statistics (CBS) data, was 4,13,397 (Wikipedia contributors, 2023). Despite the challenges of urban living, people continue to migrate to the city in search of better opportunities, resulting in overpopulation. The city was selected as the focus of this research because it exhibits urban expansion, which is linked to the reduction of urban green space.

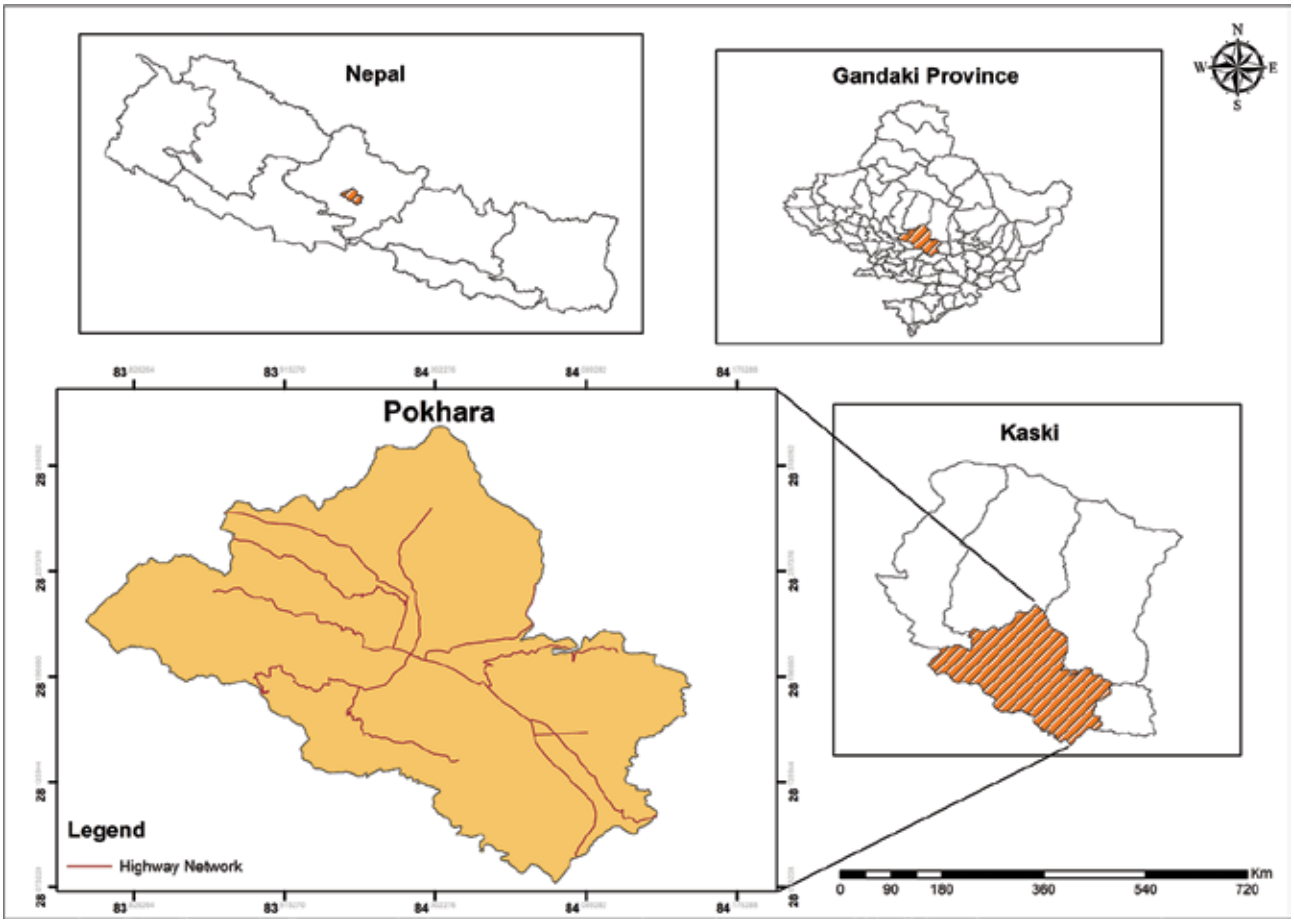

Figure 1: Location of the study area

2.2 Data collection

United States Geological Survey (USGS) Earth Explorer's Landsat collection 1 level 1 was utilized to get the Landsat data for this study which is the first and foremost step of methodological workflow as mentioned in Figure 2. Due to their availability of data different than that obtained through conventional techniques, Landsat imageries are popular in remote sensing research (Thi et al., 2018). For the years 1989, 1999, and 2009, Landsat 4-5 Thematic Mapper (TM) pictures were utilized, and for the years 2020, Landsat 8 Operational Land Imager (OLI) and Thematic Infrared Sensor (TIRS) images were used. The Landsat 4-5 and Landsat 8 utilize Worldwide Reference System (WRS)-2 data, which is used to identify the world's Landsat data by path and row numbers. Table 1 provides a description of the satellite pictures used in this study. All bands were used, apart from the panchromatic and thermal bands on Landsat 8 (with a 30-meter resolution). The images from 2000, 2010, and 2021 that were accessible were gathered to obtain cloud-free data when cloud cover ranged between 2-10%. A reference map from Google Earth Pro was used to assess the accuracy of the data classification.

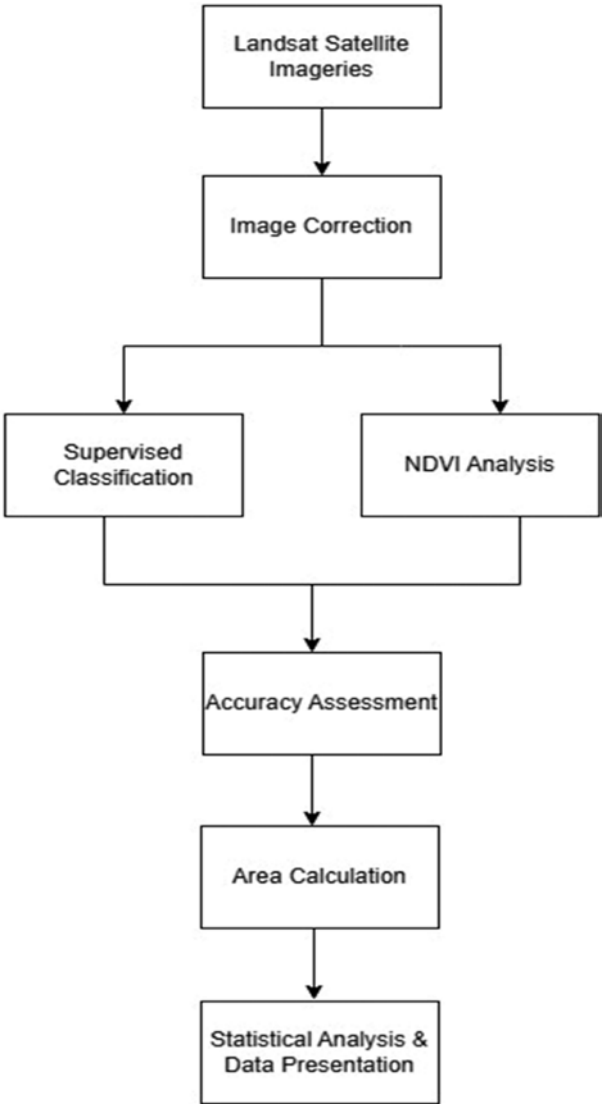

Figure 2: Methodology of the study

Table 1: Description of satellite data

Satellite	Imagery date	Reflection of bands used for NDVI	Wavelength	Resolution
Landsat 7 ETM+	2000 & 2010	Red (B3)	Landsat 7 ETM+	
Landsat 8 OLI_ TRS	2021	Red (B4) Near Infrared (B5)	B4 (0.64-0.76) B5 (0.85-0.88)	30*30 m

2.3 Data processing

2.3.1 Image pre-processing

The Top of Atmosphere (TOA) reflectance was applied to convert the Digital Number (DN) values in accordance with the standard protocols supplied by the USGS after the acquisition of Landsat-5 TM (2000 and 2010) and Landsat OLI-TIRS (2021) imagery from the USGS website (2018). Since USGS already performed geometric corrections on Level 1T products, no additional geometric correction was done for this investigation (Xiao et al., 2017). The ENVI program is used to perform radiometric correction and improve visualization. To guarantee uniformity across all satellite pictures, geo-rectification was carried out and projected to GCS WGS 1984 UTM Zone 45N (datum). The research region was masked in the images using a vector shapefile depicting the boundaries of Pokhara city.

2.3.2 Image classification

The study used supervised classification, more specifically the Maximum Likelihood supervised classification technique, which was determined to be appropriate for mapping green areas i.e., tree coverage in this project (Byomkesh et al., 2012; Dewan & Yamaguchi, 2009; Fan & Wang, 2020; Hashim et al., 2019). It is a technique for mapping land cover information that uses satellite-based remotely sensed picture data after image correction as mentioned in Figure 2. The classification was done using two separate categories: urban and green spaces, utilizing Envi 5.3 and ArcGIS 10.3. Any infrastructure besides green spaces was what the urban class stood for. As a result, various band combinations for detecting different terrain surfaces were investigated. The band combinations for healthy vegetation, natural color, and agriculture were used in the multispectral bands for the analysis of the satellite image. The infrared band combination was also employed for vegetation studies because trees mostly reflect the infrared band and absorb the red band. Using the mask tool in the Arc Toolbox, the perimeter of PMC was retrieved.

Shapefile of PMC was created using Google Earth Pro. The analysis used the WGS 1984 UTM Zone 45 projection scheme. To distinguish signature classes, color variation for various land use classes was investigated. In this study, built-up places, water, bare soil, and any other infrastructure that is not vegetation were referred to as urban and other classifications. From the two classes that were chosen, signatures were collected uniformly. For one class, several studies employed 50–100 training samples. The number of bands in the image served as the basis for selecting training examples. 10n to 100n samples were taken if there were 'n' bands (ArcMap Documentation). A total of 150–200 training samples were randomly selected from green areas to merge the samples into a single signature class that would represent the green spaces. The "non-green" or urban class was treated similarly; this procedure was repeated for each satellite image. The training pixels' points did not remain constant from year to year; instead, they changed based on the images. The raster was then transformed into a polygon, and a single coherent polygon was then obtained for each

class by using the dissolve tool. As a result, a single file with two separate classes was produced and was ready for calculation.

The area computation is quite helpful for studies on land usage. Research on land classification is insufficient without a region evaluation. The area is evaluated to distinguish between the variations of green areas with different ages. Each class area evaluation was built into a separate field on the attribute table. The "calculate geometry" tool was used to compute the area in hectares. This method was applied to all three images, each from a different year. An examination of the expansion and contraction of green spaces between 2000 and 2021 was done. For the areas, a computation was also conducted.

2.3.3 NDVI analysis

NDVI values were examined in several literatures to distinguish the healthy green, unhealthy green and non-green space (Aburas et al., 2015; Hashim et al., 2019; Julien et al., 2006; Li et al., 2015). As the NDVI values may be generated from the reflectance of healthy vegetation (Saravanan et al., 2018), it is recommended for this research due to its most widespread usage for healthy vegetation detection (Choubin et al., 2019; Dutta et al., 2021; Jiang et al., 2006). Using the surface reflectance of the visible red band and near infrared band, which are reflected by healthy plants and have wavelengths of around 0.6 m (red) and 0.9 m (near-infrared), NDVI values were determined from satellite photos (Choubin et al., 2019; Yang et al., 2021). The general formula for calculating NDVI is as follows.

$$\text{NDVI} = \frac{\text{NIR} - \text{R}}{\text{NIR} + \text{R}} \quad (1)$$

where, NIR refers near-infrared, R refers red.

For acquiring decimal values, float command was applied in this formula. Solar radiation that returns from the earth surface is sensed by Landsat sensors. Reflection of red is found from band 3 (Landsat 7) and band 4 (Landsat 8), and the reflection of near infrared bands are found from band 4 (Landsat 7) and band 5 (Landsat 8). The following equation was used for the calculation of NDVI.

$$\text{NDVI} = \frac{\text{Float (NIR -R)}}{\text{Float (NIR+R)}} \quad (2)$$

Table 2: Description of NDVI classes and values

Vegetation Classes	Description	NDVI Value
No Vegetation	Water, urban areas	<0
Unhealthy Vegetation	Unhealthy plants, bare lands, urban areas	0 to 0.2
Moderately Healthy Vegetation	Shrubs, herbs, grassland, moderately dense plants	>0.2 to 0.5
Healthy Vegetation	Dense vegetation, forest	>0.5 to 1

NDVI classes according to Buyadi et al. (2013) and Julien et al. (2006)

The NDVI readings, as described by Yengoh et al. (2016), ranged from -1 to +1, with -1 indicating the absence of vegetation and +1 indicating a thriving vegetation cover. For this experiment, four NDVI classes were established (see Table 2). The determination of NDVI thresholds was based on a review of relevant literature. The study found that vegetation with scores between 0 and 0.2 is detrimental. The range of values between > 0.2 and 0.5, which includes grasslands, cultivated fields, herbs, and shrubs, shows no significant vegetation and is considered to have "moderate vegetation" according to this study. Dense vegetation in

forested areas is indicated by values between > 0.5 and 1, which represent towering trees and dense foliage (Buyadi et al., 2013; Hashim et al., 2019; Julien et al., 2006). Areas were identified based on the NDVI class determined later.

2.4 Accuracy assessment

Google Earth Pro was used to test the accuracy of the identified imagery since it is an effective and efficient tool for time series analysis (Bishop et al., 2007; Keyhole, n.d.) and offers a high-resolution map of the earth. Every year, between 300 and 400 randomly chosen points from each ENVI class were gathered for the satellite image (2000, 2010, 2021). On Google Earth Pro, a program that simulates the real earth, the points were compared to each of the reference locations. Google Earth reference maps were used to compare the analyzed data for the years 2000, 2010, and 2021. The accuracy depended on how closely the chosen user point matched the producer points from the real world. The sample size needs to be sufficient to obtain acceptable accuracy (Landis & Koch, 1977). To calculate accuracy, the kappa coefficient and the overall user and producer accuracy were calculated. The range of the Kappa value is from -1 to +1. A Kappa value of 0.80 indicates a high degree of agreement. A value of 0.40 to 0.80 indicates a moderate level of agreement, and a value of 0.40 or less indicates a faulty level of agreement (Monserud & Leemans, 1992). The first equation calculates overall accuracy. User accuracy is also referred to as error of commission, while producer correctness is known as error of omission. Eqs. (4) and (5) can be used to calculate the producer and user accuracy, respectively.

$$\text{Overall accuracy} = \frac{\text{Total number of correctly classified pixel (Diagonal)}}{\text{Total number of reference pixel}} * 100 \quad (3)$$

$$\text{Producer's accuracy} = \frac{\text{Number of correctly classified pixel in each category}}{\text{Total number of reference pixel in that category (Column total)}} * 100 \quad (4)$$

$$\text{User Accuracy} = \frac{\text{Number of correctly classified pixel in each category}}{\text{Total number of classified pixel in that category (Row total)}} * 100 \quad (5)$$

2.4.1 Kappa coefficient

A statistical method for evaluating how successfully classifications have been made is the kappa coefficient. It is more realistically accurate in case the higher the kappa value. Different researchers employ a variety of formulas.

$$\text{Kappa Coefficient} = \frac{(TS * TCS) - \Sigma(Col.total * row.total)}{T S 2 - \Sigma(Col.total / row.total)} * 100 \quad (6)$$

here,

TS = Total number of samples taken

TCS = Total number of correct Samples

Col. total = Total sample in each column

Row total = Total sample in each row

3. Results and Discussion

3.1 Green space status

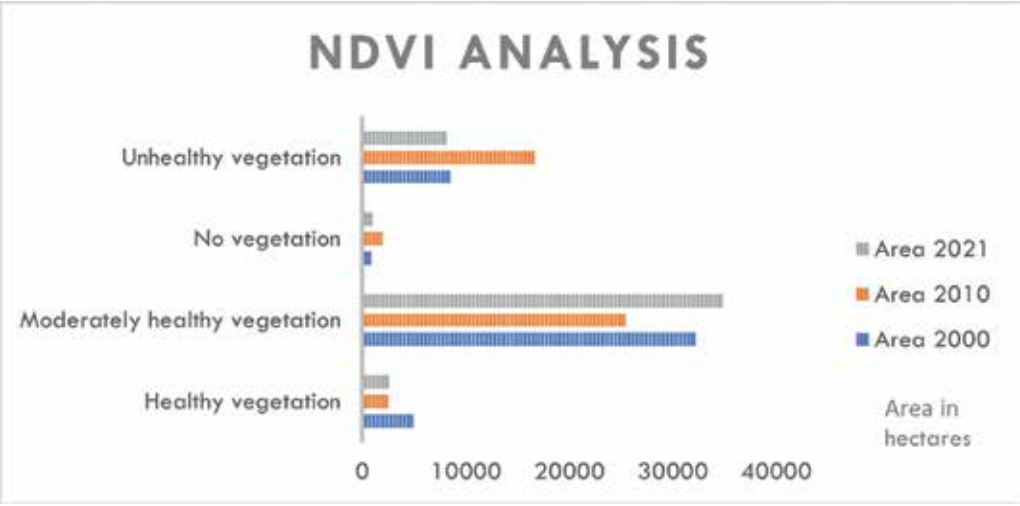

Figure 3: Comparison of different types of vegetation

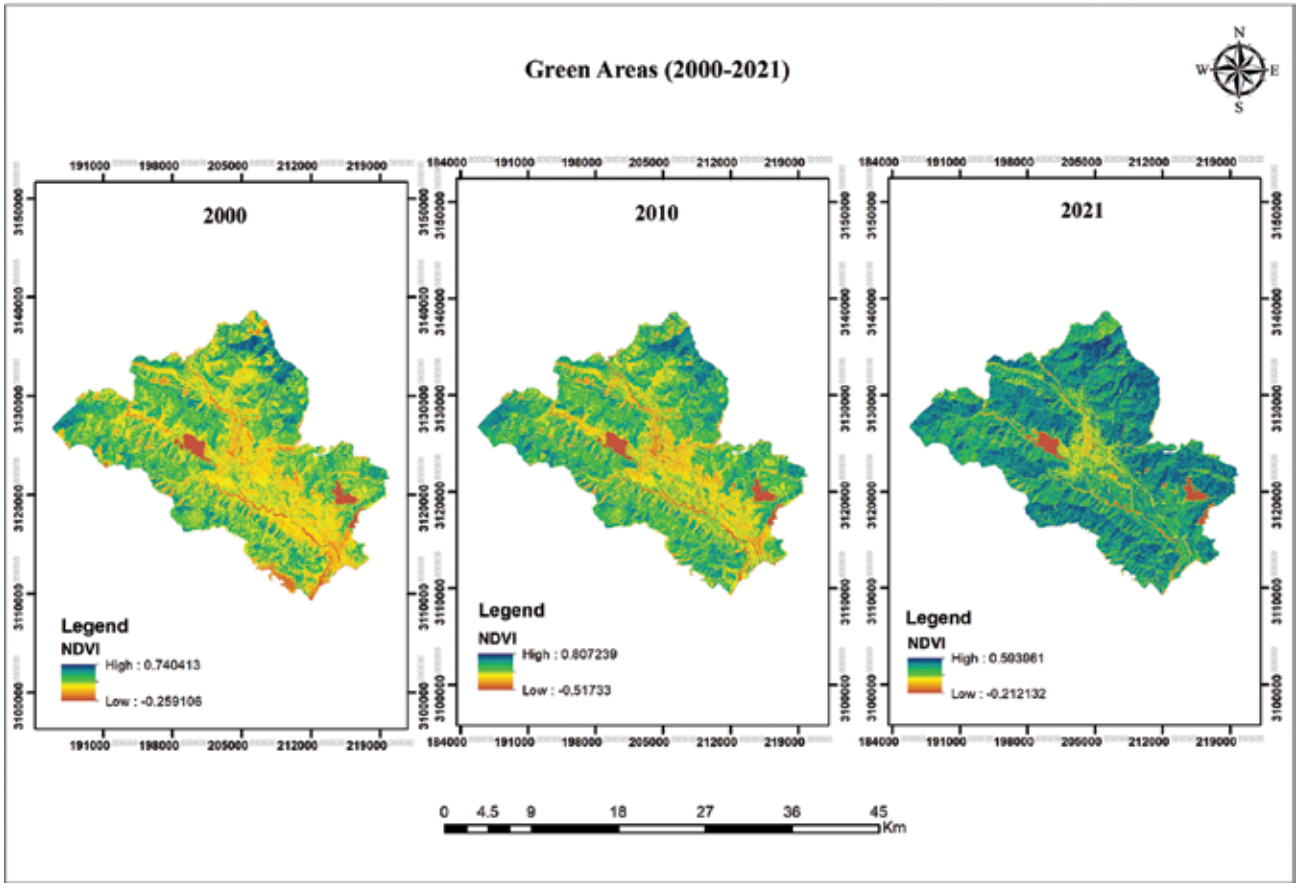

Figure 4: Spatiotemporal evaluation of NDVI

This study examined the changes in urban green space within PMC from 2000 to 2021, under the influence of urbanization. GIS and remote sensing (RS) techniques were used to analyze fluctuations in the number of green spaces, confirming the research hypothesis. The NDVI results revealed that in 2000, the highest number of healthy green spaces was 4926 hectares (10.61%), which decreased over time. However, moderately healthy vegetation increased from 2000 to 2021, as depicted in Figure 3. There was also an increase in grassland, mainly in hilly or remote areas, as residents moved to city areas and agricultural land was converted to grassland. Additionally, deforestation in suburban areas contributed to the growth of grassland resulting in an increase in green space within PMC. However, in the core city regions of PMC, the amount of non-vegetated or urban bare lands increased.

No-vegetation areas generally resemble swamps, lakes, and other bodies of water, while some structures may also be included in this category. Buildings, sand, bare soils, and other similar materials make up most of the bare land class. Any green vegetation, including small plants, grasses, herbs, shrubs, and regions with moderate and sparse vegetation is considered a moderate green space in this context. Large trees, lush foliage, and forest lands — all of which have become increasingly rare over time — are the main characteristics of healthy green areas. The spatiotemporal evaluation of NDVI of PMC is shown in Figure 4.

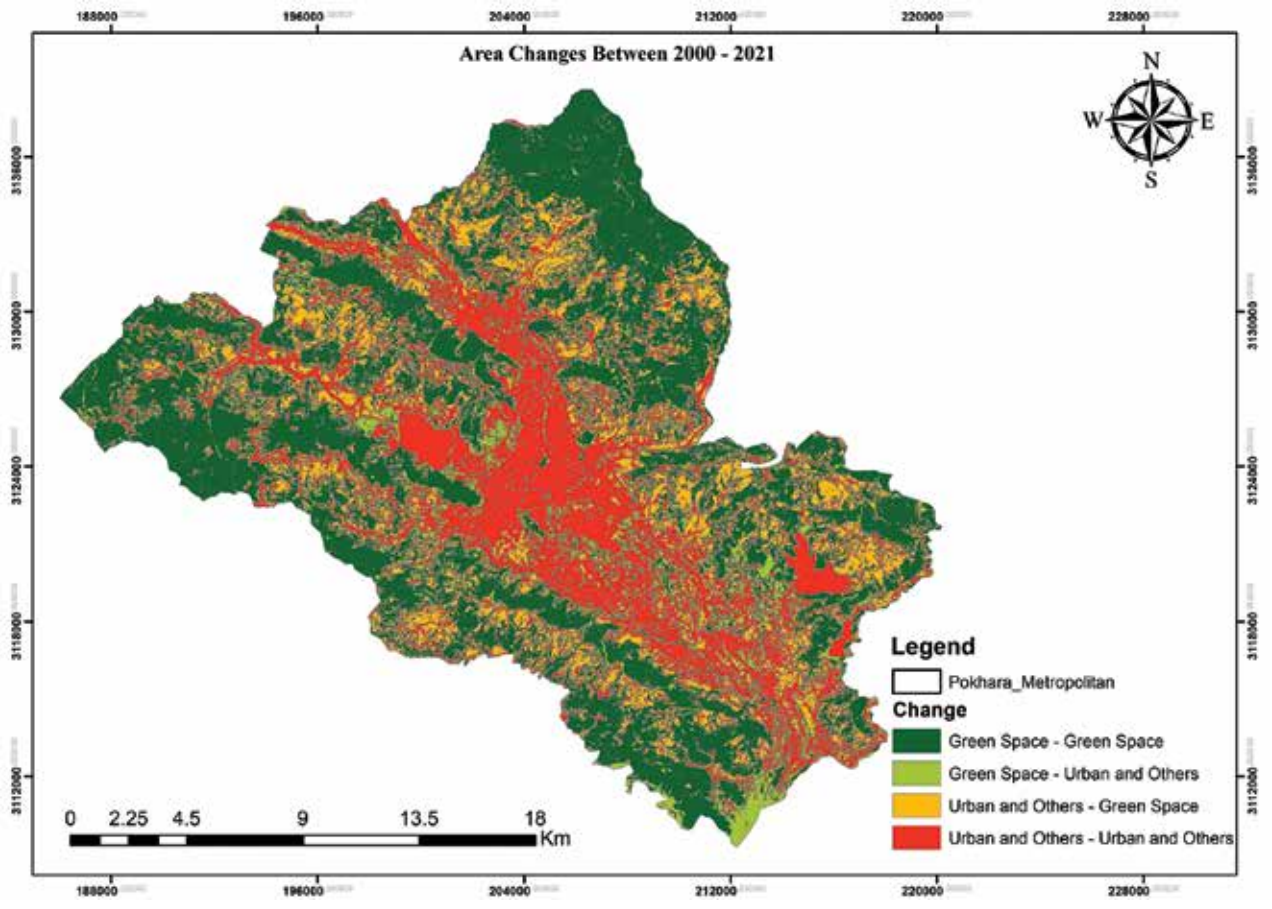

Figure 5: Spatiotemporal evaluation of green space

The study detected a trend of urban green space transformation in which area changes were calculated from green space to green space, urban areas to urban areas, and vice versa between 2000 and 2021. The

transformation of urban green space in PMC exhibited two distinct patterns. Urban areas in core city regions expanded, resulting in the conversion of 5432.15 hectares (11.70%) of green space. In contrast, nearby sub-urban areas, such as Bhadauri Tamagi, Kalika, and Kristi, experienced an increase in green space, with 8637.62 hectares (18.60%) of total area converted due to migration to core city areas and the conversion of agricultural land into dense grasslands as shown in Figure5.

The study examines how the transformation of urban green spaces is related to the spatial orientation of urban areas. It reveals that built-up areas are mainly concentrated along major highways and within the central region. The study finds that urbanization has predominantly occurred along three primary highways: Siddhartha, Prithvi, and Baglung, which run in the south-east, north-east, and north-west directions, respectively. As people from rural areas move closer to urban centers, their location preferences are also apparent. For example, migrants from Syangja, located south of the PMC, tend to settle in the ward-17 region, located in the south-eastern direction of the PMC or Siddhartha highway. Migrants from Baglung and Parbat, located to the west of the PMC, tend to settle in the Hemja and Lamachour region, located to the north-west of the PMC or Baglung highway. Similarly, migrants from Tanahun, Lamjung, and other areas located to the east of the PMC tend to settle in the north-eastern direction of the PMC or Prithvi highway. Additionally, the study notes that urban growth in cities often follows the sides of major highways, rivers, and lakes, as well as the central area's densification.

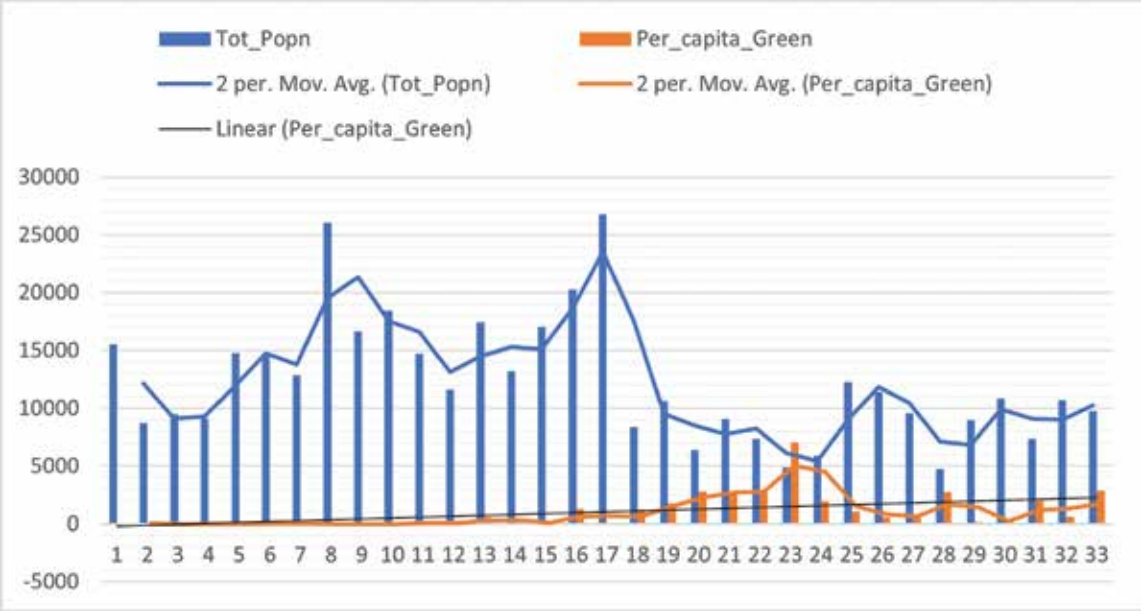

Figure 6: Correlation graph between per capita green and population density

The study indicates a negative correlation between population and per capita green, with wards one to seventeen and wards 26, 27, and 29 exhibiting low per capita green, while the remaining wards show high per capita green. The trend line of Figure 6 depicts a two-point moving average in both per capita green and total population for each ward. The Pokhara metropolitan area was created through the merger of the former Pokhara sub-metro, Lekhnath Municipality, and neighboring VDCs. The correlation graph reveals that the former sub-metropolitan ward has a high population density and low per capita green, while the former VDC wards exhibit low population density and high per capita green.

3.2 Accuracy assessment

Typically, accuracy assessments involve comparing data against reference data that is assumed to be correct. In the year 2000, approximately 390 training samples were taken, with user accuracy and producer accuracy for green space measuring at 79.17% and 95%, respectively, while the same values for urban space were 93.28% and 73.54%, respectively. Similarly, in 2010, around 345 training sample points were taken as shown in Figure 7 resulting in user accuracy and producer accuracy of 74.8% and 67.58% for green space, respectively. The average user accuracy and producer accuracy for the year 2021 were 84.63% and 86.76% respectively. A Kappa value of 0.68 was obtained for the year 2000 while the Kappa values for 2010 and 2021 were 0.52 and 0.69 respectively. Kappa values above 0.6 are considered acceptable and good values. Overall accuracy was calculated, resulting in good results of 84.57%, 76.74%, and 84.43% of three different images sequentially. The analysis accuracy ranged from moderate to highly accurate, as defined by Monserud and Leemans (1992). While overall and total accuracy are significant, they may not always reflect the actual situation, which is why producer and user accuracy were also calculated and enlisted in Table 3. The average overall accuracy of all three imageries was found to be 81.91%.

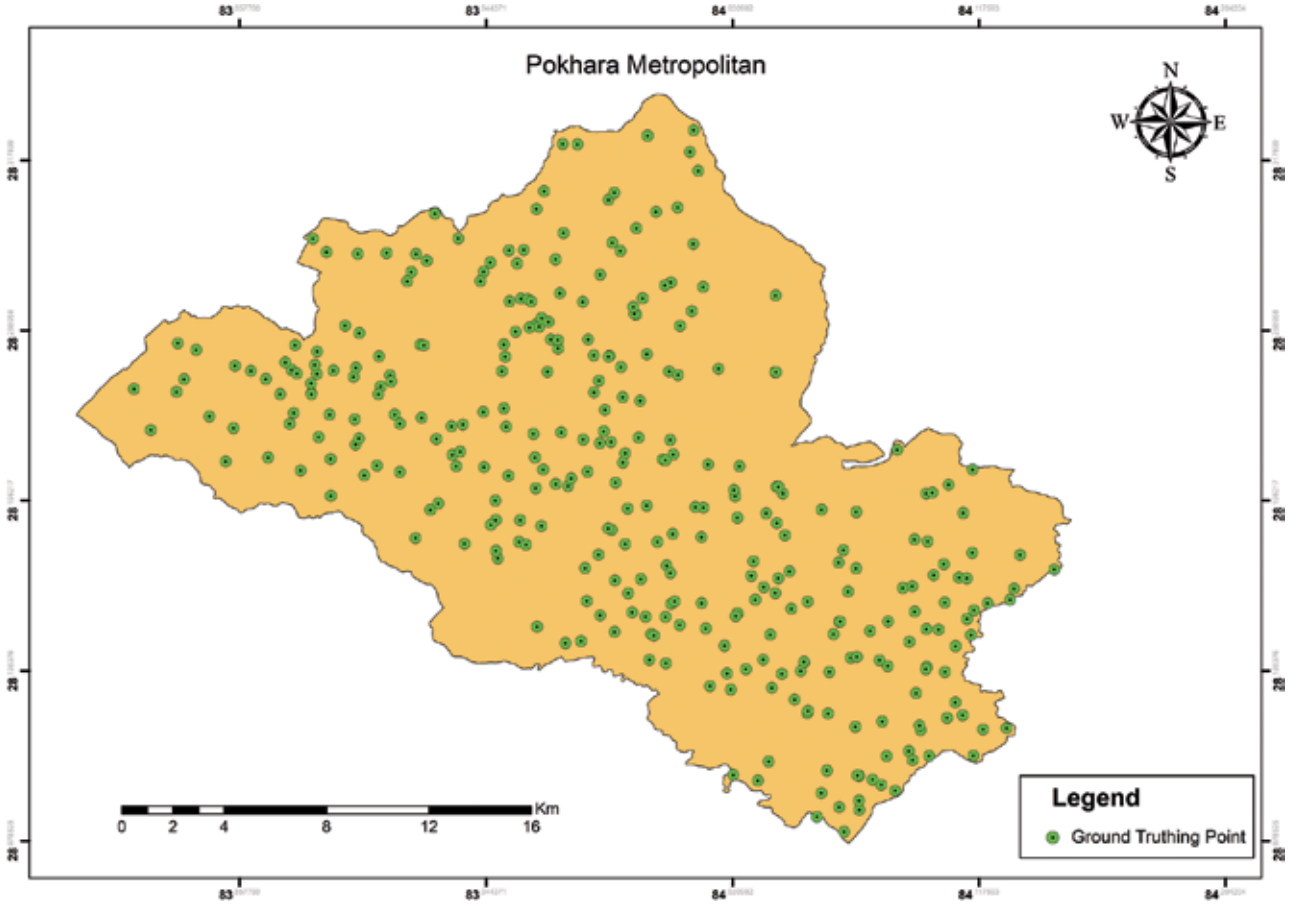

Figure 7: Ground truthing points map

Table 3: Overall calculation of accuracy and Kappa coefficient

Type	Year 2000				Year 2010				Year 2021			
	PA	UA	Overall	Kappa	PA	UA	Overall	Kappa	PA	UA	Overall	Kappa
Green Space	95	79.17	84.57	0.68	67.58	74.80	76.74	0.52	79.48	86.11	84.43	0.69
Urban and Others	73.54	93.28			83.42	77.93			94.04	83.15		

where, PA = Producers Accuracy, UA = User Accuracy

3.3 Discussion

Based on satellite imagery classification and NDVI methods, it is estimated that Pokhara's green space has been undergoing changes with a gradual decline in green space in the city's core areas while there has been an increase in sub-urban and remote areas of PMC as agricultural land has been converted into grassland. This change is due to the migration of residents to the city's core areas, where housing is available. As a result, the area of healthy vegetation decreased from 4926 hectares to 2535 hectares, while moderately healthy vegetation increased. Additionally, the area lacking vegetation, such as urban areas, increased from 838 hectares to 1007 hectares. Migration is one of the primary causes of the urban population increase in Pokhara. These findings are like the latest data released by the Forest Research and Training Center (FRTC) which shows that Nepal's forest area increased by 1.7 percent and agricultural land shrunk by 2.1 percent due to the expansion of built-up areas from 2000 to 2019 (FRTC, 2022). A similar study in PMC by Raut et al. (2020) has found that over the past 18 years, there has been a steady rise in the amount of developed and forested land with a corresponding decrease in open spaces and agricultural land. The expansion of urbanization is primarily concentrated in city areas and is encroaching on previously open spaces. The devastation caused by the 2015 earthquake also contributed to the loss of open spaces (Raut et al., 2020). Despite not being able to meet the demands of the growing urban population, the city's core areas continue to attract people as it is the capital of the province and district with many government offices and business hubs located in the area. Pokhara has also become an essential location for the informal economy which attracts migrants from rural areas to the metropolitan areas.

4. Conclusions

The objective of this study was to examine the size of green spaces in PMC in the last two decades. The results indicate that the amount of green space decreased significantly in central city areas due to the expansion of urban infrastructure. However, in the city's outlying and suburban areas, the amount of green space increased as agricultural fields were converted into dense grasslands. To promote the growth of urban green spaces in the central city region, it is the responsibility of government agencies to identify, monitor, and safeguard potential sites. Many cities and metropolitan areas recognize the value of urban green spaces and are prioritizing their development to achieve resilient urban development plans that encompass environmental, social, economic, cultural, and disaster risk reduction strategies. Urban open green spaces offer a range of cross-cutting ecological benefits that can enhance overall building resilience.

Acknowledgements

Authors would like to express our sincere gratitude to Assoc. Prof. Dr. Krishna Prasad Bhandari and Asst.

Prof. Bikash Sherchan, Tribhuvan University, Institute of Engineering, Pashchimanchal Campus for their continuous guidance and advice throughout the course of this study.

Declaration of Competing Interest

The authors declare that they have no known competing financial interests or personal relationships that could have appeared to influence the work reported in this paper.

References

Abebe, M. T., & Megento, T. L. (2017). Urban green space development using GIS-based multi-criteria analysis in Addis Ababa metropolis. *Applied Geomatics*, *9*(4), 247–261. https://doi.org/10.1007/s12518-017-0198-7

Aburas, M. M., Abdullah, S. H., Ramli, M. F., & Ash'aari, Z. H. (2015). Measuring Land Cover Change in Seremban, Malaysia Using NDVI Index. *Procedia Environmental Sciences*, *30*, 238–243. https://doi.org/10.1016/j.proenv.2015.10.043

Bauwelinck, M., Casas, L., Nawrot, T. S., Nemery, B., Trabelsi, S., Thomas, I., Aerts, R., Lefebvre, W., Vanpoucke, C., Van Nieuwenhuyse, A., Deboosere, P., & Vandenheede, H. (2021). Residing in urban areas with higher green space is associated with lower mortality risk: A census-based cohort study with ten years of follow-up. *Environment International*, *148*, 106365. https://doi.org/10.1016/j.envint.2020.106365

Bishop, Y. M., Holland, P. W., & Fienberg, S. E. (2007). Discrete multivariate analysis theory and practice. In *Discrete Multivariate Analysis Theory and Practice*. https://doi.org/10.1007/978-0-387-72806-3

Byomkesh, T., Nakagoshi, N., & Dewan, A. M. (2012). Urbanization and green space dynamics in Greater Dhaka, Bangladesh. *Landscape and Ecological Engineering*, *8*(1), 45–58. https://doi.org/10.1007/s11355-010-0147-7

Choubin, B., Soleimani, F., Pirnia, A., Sajedi-Hosseini, F., Alilou, H., Rahmati, O., Melesse, A. M., Singh, V. P., & Shahabi, H. (2019). Effects of drought on vegetative cover changes: Investigating spatiotemporal patterns. In *Extreme Hydrology and Climate Variability: Monitoring, Modelling, Adaptation and Mitigation* (Vol. 2). Elsevier Inc. https://doi.org/10.1016/B978-0-12-815998-9.00017-8

Davies, R. G., Barbosa, O., Fuller, R. A., Tratalos, J., Burke, N., Lewis, D., Warren, P. H., & Gaston, K. J. (2008). City-wide relationships between green spaces, urban land use and topography. *Urban Ecosystems*, *11*(3), 269–287. https://doi.org/10.1007/s11252-008-0062-y

Dewan, A. M., & Yamaguchi, Y. (2009). Land use and land cover change in Greater Dhaka, Bangladesh: Using remote sensing to promote sustainable urbanization. *Applied Geography*, *29*(3), 390–401. https://doi.org/10.1016/j.apgeog.2008.12.005

Dutta, S., Rehman, S., Chatterjee, S., & Sajjad, H. (2021). Analyzing seasonal variation in the vegetation cover using NDVI and rainfall in the dry deciduous forest region of Eastern India. In *Forest Resources Resilience and Conflicts* (Issue June). https://doi.org/10.1016/B978-0-12-822931-6.00003-4

Fan, C., & Wang, Z. (2020). Spatiotemporal characterization of land cover impacts on urban warming: A spatial autocorrelation approach. *Remote Sensing*, *12*(10), 1–17. https://doi.org/10.3390/rs12101631

Hashim, H., Abd Latif, Z., & Adnan, N. A. (2019). Urban vegetation classification with NDVI threshold value method with very high resolution (VHR) pleiades imagery. *International Archives of the Photogrammetry, Remote Sensing and Spatial Information Sciences - ISPRS Archives*, *42*(4/W16), 237–240. https://doi.org/10.5194/isprs-archives-XLII-4-W16-237-2019

Image classification using the ArcGIS Spatial Analyst extension —ArcMap Documentation, E. 2021). (n.d.). *Image classification using the ArcGIS Spatial Analyst extension—ArcMap | Documentation*. Retrieved November 12, 2022, from https://desktop.arcgis.com/en/arcmap/latest/extensions/spatial-analyst/image-classification/image-classification-using-spatial-analyst.htm

Jiang, Z., Huete, A. R., Chen, J., Chen, Y., Li, J., Yan, G., & Zhang, X. (2006). Analysis of NDVI and scaled difference vegetation index retrievals of vegetation fraction. *Remote Sensing of Environment*, *101*(3), 366–378. https://doi.org/10.1016/j.rse.2006.01.003

Julien, Y., Sobrino, J. A., & Verhoef, W. (2006). Changes in land surface temperatures and NDVI values over Europe between 1982 and 1999. *Remote Sensing of Environment*, *103*(1), 43–55. https://doi.org/10.1016/j.rse.2006.03.011

Keyhole, I. (n.d.). *Google Earth Pro – A useful tool for Environmental Practitioners - Integrate Sustainability*. Retrieved November 12, 2022, from https://www.integratesustainability.com.au/2017/08/24/google-earth-pro-a-useful-tool-for-environmental-practitioners/

Kuang, W., Zhang, S., Li, X., & Lu, D. (2021). A 30 m resolution dataset of China's urban impervious surface area and green space, 2000-2018. *Earth System Science Data*, *13*(1), 63–82. https://doi.org/10.5194/essd-13-63-2021

Landis, J. R., & Koch, G. G. (1977). Landis amd Koch1977_agreement of categorical data. *Biometrics*, *33*(1), 159–174.

Li, W., Saphores, J. D. M., & Gillespie, T. W. (2015). A comparison of the economic benefits of urban green spaces estimated with NDVI and with high-resolution land cover data. *Landscape and Urban Planning*, *133*, 105–117. https://doi.org/10.1016/j.landurbplan.2014.09.013

Monserud, R. A., & Leemans, R. (1992). Comparing global vegetation maps with the Kappa statistic. *Ecological Modelling*, *62*(4), 275–293. https://doi.org/10.1016/0304-3800(92)90003-W

Montandon, L. M., & Small, E. E. (2008). The impact of soil reflectance on the quantification of the green vegetation fraction from NDVI. *Remote Sensing of Environment*, *112*(4), 1835–1845. https://doi.org/10.1016/j.rse.2007.09.007

Morris, K. I., Chan, A., Ooi, M. C., Oozeer, M. Y., Abakr, Y. A., & Morris, K. J. K. (2016). Effect of vegetation and waterbody on the garden city concept: An evaluation study using a newly developed city, Putrajaya, Malaysia. *Computers, Environment and Urban Systems*, *58*, 39–51. https://doi.org/10.1016/j.compenvurbsys.2016.03.005

Nawar, N., Sorker, R., Chowdhury, F. J., & Mostafizur Rahman, M. (2022). Present status and historical changes of urban green space in Dhaka city, Bangladesh: A remote sensing driven approach. *Environmental Challenges*, *6*(December 2021), 100425. https://doi.org/10.1016/j.envc.2021.100425

Pokhrel, S. (2019). Green space suitability evaluation for urban resilience: an analysis of kathmandu metropolitan city, nepal. *Environmental Research Communications*, *1*(10). https://doi.org/10.1088/2515-7620/ab4565

Raut, S. K., Chaudhary, P., & Thapa, L. (2020). Land Use/Land Cover Change Detection in Pokhara Metropolitan, Nepal Using Remote Sensing. *Journal of Geoscience and Environment Protection*, *08*(08), 25–35. https://doi.org/10.4236/gep.2020.88003

Richards, J. A. (2006). *Richards, J. , Jia, X. , 2006. Remote Sensing Digital Image Analysis: An Introduction. Springer 4, Berlin* .

Rukiye Duygu Çay and Fatma Aşılıoğlu. (2016). Benefits of Urban Green Spaces for Citizens : Ankara Case Study „ Ecology of Urban Areas " 2014 Benefits of Urban Green Spaces for Citizens : Ankara Case Study. *Ecology of Urban Areas 2014*, *April*, 1–8.

Rwanga, S. S., & Ndambuki, J. M. (2017). Accuracy Assessment of Land Use/Land Cover Classification Using Remote Sensing and GIS. *International Journal of Geosciences*, *08*(04), 611–622. https://doi.org/10.4236/ijg.2017.84033

Saravanan, S., Jegankumar, R., Selvaraj, A., Jacinth Jennifer, J., & Parthasarathy, K. S. S. (2018). Utility of Landsat Data for Assessing Mangrove Degradation in Muthupet Lagoon, South India. In *Coastal Zone Management: Global Perspectives, Regional Processes, Local Issues*. Elsevier Inc. https://doi.org/10.1016/B978-0-12-814350-6.00020-3

Shih, W. (2017). Greenspace patterns and the mitigation of land surface temperature in Taipei metropolis. *Habitat International*, *60*, 69–80. https://doi.org/10.1016/j.habitatint.2016.12.006

Tew, Y. L., Tan, M. L., Samat, N., & Yang, X. (2019). Urban expansion analysis using landsat images in Penang, malaysia. *Sains Malaysiana*, *48*(11), 2307–2315. https://doi.org/10.17576/jsm-2019-4811-02

Thi, T., An, T., Lam, L. T., Hoa, N. H., Son, L. T., & Hung, N. Van. (2018). Using Landsat Imageries for Particle Pollution Mapping. *Management of Forest Resources and Environment*, *5*, 53–61.

Wolch, J. R., Byrne, J., & Newell, J. P. (2014). Urban green space, public health, and environmental justice: The challenge of making cities "just green enough." *Landscape and Urban Planning*, *125*, 234–244. https://doi.org/10.1016/j.landurbplan.2014.01.017

Xiao, Y., Ouyang, Z., Zhang, Z., & Xian, C. (2017). Comparação entre algoritmos de remoção de neblina e seu impacto na acurácia da classificação de imagens Landsat. *Boletim de Ciencias Geodesicas*, *23*(1), 55–71. https://doi.org/10.1590/S1982-21702017000100004

Yang, L., Yu, K., Ai, J., Liu, Y., Lin, L., Lin, L., & Liu, J. (2021). The influence of green space patterns on land surface temperature in different seasons: A case study of fuzhou city, china. *Remote Sensing*, *13*(24). https://doi.org/10.3390/rs13245114

Zhang, X., Hu, Y., Zhuang, D., Qi, Y., & Ma, X. (2009). NDVI spatial pattern and its differentiation on the Mongolian Plateau. *Journal of Geographical Sciences*, *19*(4), 403–415. https://doi.org/10.1007/s11442-009-0403-7

Zhou, X., & Wang, Y. C. (2011). Spatial-temporal dynamics of urban green space in response to rapid urbanization and greening policies. *Landscape and Urban Planning*, *100*(3), 268–277. https://doi.org/10.1016/j.landurbplan.2010.12.013